AIAA JOURNAL
Vol. 37, No. 4, April 1999

Convex/Probabilistic Models of Uncertainties in Geometric Imperfections of Stiffened Composite Panels

M. A. Elseifi,* Z. Gürdal,† and E. Nikolaidis‡
Virginia Polytechnic Institute and State University, Blacksburg, Virginia 24061

Thin-walled stiffened composite panels, which are among the most utilized structural elements in engineering, possess the unfortunate property of being highly sensitive to geometric imperfections. Existing analysis codes can predict the buckling load of a structure with specified initial imperfections. However, it is impossible to determine the amplitude and shape of imperfections of nonexistent composite panels that are only being designed. This is due to a variety of uncertainties that are involved in fabrication of panels. Because of the very nature of the manufacturing processes, it is hard to imagine that a given process could ever produce two identical panels. Currently, however, rather than analyzing the manufacturing processes that lead to imperfections, panels are typically designed using probabilistic models to account for the uncertainties in imperfections. An efficient approach is presented that employs a convex model of the uncertainties in the imperfections. This approach can replace the computationally expensive probabilistic approach typically used in the study of imperfection sensitive structures. Several example problems are solved to show the accuracy of the predictions of the convex model. A Monte Carlo simulation has also been performed to validate the results obtained by the convex model and show the effort and cost reductions obtained by the use of such models.

Nomenclature

A_{ij}	= Fourier coefficients
h	= blade height
L	= panel length
N_D	= design load
N_L	= limit load
$\boldsymbol{q}$	= vector of modal imperfection amplitudes
q_i	= modal amplitude (mode i)
q_i^0	= modal imperfection amplitude
$\boldsymbol{q}^0$	= nominal imperfection profile
$\boldsymbol{q}_1^*, \boldsymbol{q}_2^*$	= weakest and strongest panel profiles
t	= ply thickness
$\{u\}$	= panel displacement vector
$\{u_L\}$	= panel linear displacement vector
W	= panel width
x, y	= local space coordinates
$\bar{x}, \bar{y}$	= panel global coordinate system
Z	= ellipsoidal set
α	= size parameter
γ	= Lagrange multiplier
$\delta(x, y)$	= deviation of the panel from its nominal shape at point (x, y)
$\eta(\boldsymbol{q})$	= elastic limit load for a panel with initial imperfection profile $\boldsymbol{q}$
Λ	= panel's buckling load
φ_{ij}	= complete set of functions
$\boldsymbol{\omega}$	= vector of semiaxis lengths

I. Introduction

THE design and analysis of compressively loaded stiffened composite panels has been studied by many investigators,[1,2] and it is well known that the elastic limit load of a panel is greatly affected by the initial imperfections in the panel shape.[3] The load vs end-shortening response (normalized with respect to their critical values) of a simply supported stiffened panel, for example, is shown in Fig. 1. The solid lines in Fig. 1 correspond to perfect panel behavior, whereas the dashed lines are for imperfect panels. The geometrically nonlinear behavior observed in Fig. 1 can be classified into three general types: short-wavelength postbuckling, Euler postbuckling, and modal interaction. For the short-wavelength postbuckling, the panel buckles into half-wavelengths, which are approximately equal to the width between stiffeners, and is capable of carrying loads greater than its buckling load. For Euler (global) postbuckling, the panel buckles into one half-wavelength along its length, and its load-carrying capabilities remain essentially neutral after buckling. The modal interaction is a case in which the short-wavelength and Euler modes have critical loads of almost equal values. In this case, the panel is unable to carry loads greater than its buckling load. Moreover, the panel becomes extremely sensitive to imperfections, reaching an elastic limit load well below the predicted buckling load. Initial imperfections are the primary source of discrepancy between experimental failure loads and loads predicted on the basis of linear structural analysis.

Historically, engineers have employed empirical knockdown factors to account for the large discrepancy between theoretical and experimental values of buckling and elastic limit loads. The knockdown factor, when multiplied by the classical buckling load for the perfect structure, yields an estimated lower bound of the buckling load for the imperfect structure. The knockdown factors are often determined experimentally for a range of distinct structures, materials, and manufacturing processes. Such an approach has several drawbacks, such as the need to constantly update the knockdown factor to include new experimental results.

A more sophisticated approach will be to use finite element techniques for the nonlinear analysis and design of stiffened panels with imperfections. However, the high computational cost associated with this approach prevents their use in cases requiring repetitive analyses, such as optimization problems. Several approximate methods using analytical or semi-analytical approaches have been developed to obtain a more economical way of taking into account the effects of geometrical imperfections and the nonlinearities. An example is PANDA2 by Bushnell.[4]

Another approximate semi-analytical method was recently developed for geometrically nonlinear analysis of thin-walled composite panels.[2] The analysis is capable of predicting the nonlinear postbuckling stresses and deformations, elastic limit points, and imperfection sensitivity of panels in a cost-effective manner. The panel geometries that can be analyzed are composed of linked prismatic plate strips (for example, see Fig. 2). The panels may be subjected to

Received March 9, 1998; revision received Nov. 20, 1998; accepted for publication Nov. 29, 1998.

*Graduate Research Assistant, Department of Aerospace and Ocean Engineering. Student Member AIAA.

†Professor, Departments of Aerospace and Ocean Engineering and of Engineering Science and Mechanics. Associate Fellow AIAA.

‡Associate Professor, Department of Aerospace and Ocean Engineering.

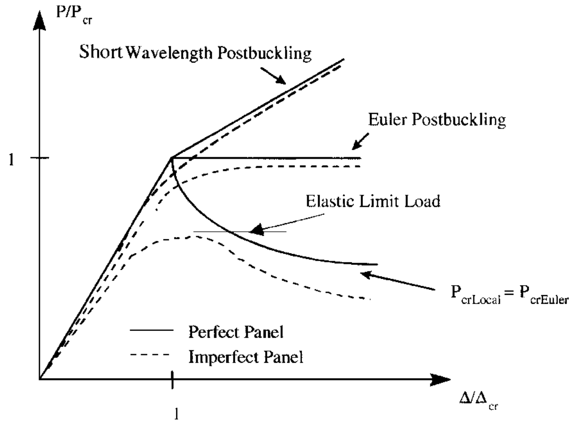

Fig. 1 Nonlinear elastic behavior of stiffened panels.

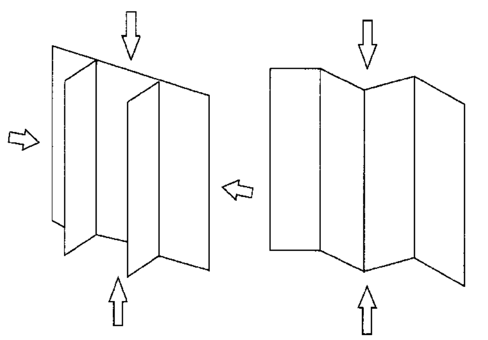

Fig. 2 Typical compressively loaded prismatic linked-plate structures.

a variety of load cases, including uniaxial loads, combined in-plane axial loads, pressure, and temperature. The method was developed as an extension to the buckling analysis code VIPASA and uses buckling eigenfunctions, calculated by VIPASA[5] as the primary displacement shape functions for the nonlinear analysis. It has been incorporated into a Fortran code, NLPAN, and is suitable for optimum design problems because of its low computational cost.

Although appropriate tools capable of incorporating initial imperfection into the analysis exist, the use of such tools to design panels is not straightforward. One of the dilemmas is the shape and magnitude of imperfections. The exact shape of imperfections is known only for existing panels. If, on the other hand, we are interested in designing a panel, we will have no information about the magnitude and shape of the imperfections in that nonexistent panel. One way to handle this situation has been to assume the worst-case scenario for the shape of imperfections with magnitudes with built-in uncertainty.

A natural way to deal with uncertainty in the initial imperfections is to employ a stochastic approach. Bolotin[6] presented a probabilistic analysis that treated initial imperfections as random variables with a specified joint distribution. Another treatment of the imperfections is due to Budiansky and Hutchinson,[7] who represented the imperfections as random fields with given mean and autocorrelation function. These approaches have been bridged by Elishakoff,[8] who used the Monte Carlo simulation method.

Probabilistic analysis typically treats the initial imperfections as random functions of the space coordinates x and y of the panel. Let $\delta(x, y)$ represent the deviation of the panel from its nominal shape at point x, y. If one knows an analytical relation between the buckling load Λ and the initial imperfection function $\delta(x, y)$,

$$\Lambda = \Psi[\delta(x, y)]$$

then one can relate the probabilistic characteristics of Λ with those of δ, resulting in an expression for the probability density of the buckling load. Except for the simplest cases, there is no analytical relation of this type available in the literature. Usually, the initial imperfection function is expanded in a Fourier series:

$$\delta(x, y) = \sum_{i,j} A_{ij}\varphi_{ij}(x, y)$$

Then available computer codes yield relations of the type

$$\Lambda = \Psi(A_{ij})$$

The aim of this study is to exploit partial information (which is usually all that is available) about the initial imperfection of stiffened panels, to determine their buckling loads. Explicitly, the minimum buckling load will be determined as a function of parameters that characterize the range of possible initial imperfection profiles of the panel. Nonprobabilistic convex models of uncertainty in the initial imperfections will be employed. The uncertainty in the initial imperfection profiles will be quantified in terms of the variability of the modal amplitudes of those profiles. The amplitudes of the first N most significant mode shapes are assumed to fall in an ellipsoid set in the N-dimensional Euclidean space. The minimum elastic limit load is then evaluated as a function of the shape of the ellipsoid. The convex model of uncertainty was used by Lindberg[9] in the analysis of radial pulse buckling of shells. Ben-Haim and Elishakoff[10] used it in the analysis of static axial buckling of shells and in other applications.[11]

A more detailed discussion of the panel geometry, along with schemes used for designing panels for imperfections, and the suggested new scheme are discussed in Sec. II. Section III presents the convex model employed along with the mathematical analysis involved in predicting the weakest panel profile. Predictions of the convex model are compared with those obtained by direct minimization in Sec. IV. Finally, a probabilistic analysis of the problem is presented in Sec. V to demonstrate the validity of the results obtained by the convex model and their simplicity compared with the traditional stochastic approach.

II. Design Problem

The panel configuration used in this study is shown in Fig. 3. The panel is composed of thin rectangular plate strips connected along their longitudinal sides. The panel model contains three plate strips, two internal node lines (2 and 3), and two boundary node lines (1 and 4). The boundary conditions at the longitudinal ends of the panel ($\bar{x} = 0$ and L) and the external boundary node lines ($\bar{y} = 0$ and B) are assumed to be simply supported. The panel is made of graphite/epoxy laminates with the following material properties: $E_1 = 20.00 \times 10^6$ psi, $E_2 = 1.30 \times 10^6$ psi, $G_{12} = 1.03 \times 10^6$ psi, and $\nu_{12} = 0.30$. The panel dimensions are length $L = 48.1$ in., width $W = 6.28318$ in., and blade height $h = 1.42189$ in. The skin laminate stacking sequences are $[45/-45/90_2/0]$ and $[45/-45/90/0_{10}]$, respectively, with ply thicknesses of $t = 0.006$ in. The panel is subjected to axial loading in the x direction only; $N_x = 1000$ psi. Neither out-of-plane pressure nor thermal loadings are applied.

The analysis assumes that, in the postbuckling load regime, the panel displacements have the following form:

$$\{u\} = \lambda\{u_L\} + q_i\{u_i\} + q_i q_j\{u_{ij}\}, \qquad i, j = 1, 2, \ldots$$

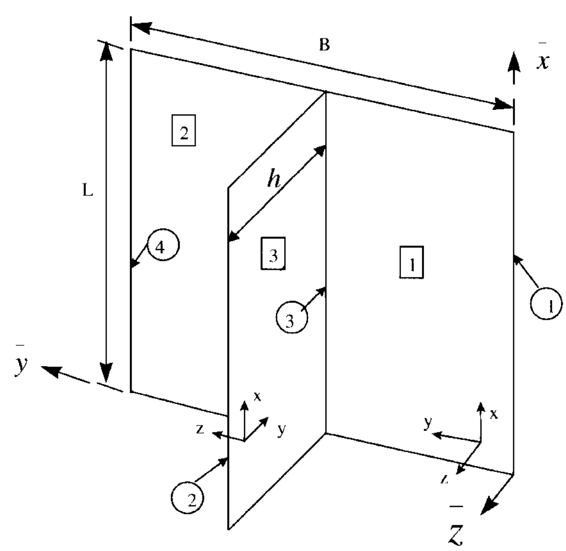

Fig. 3 Stiffened panel showing plate strip and labeling conventions.

where summation over i and j is implied and $\{u\}$ is the vector of displacements in the x, y, and z directions. Displacements are represented as a sum of linear unbuckled contributions $\{u_L\}$ and a truncated perturbation expansion in terms of modal amplitudes q_i. The q_i are the unknown amplitude multipliers for the buckling mode shapes $\{u_i\}$, which are used to represent the displacements in the nonlinear regime. The magnitudes of q_i are load dependent and determine the degree of influence their respective buckling modes have on the response of the panel. Displacement contributions of second order in the modal amplitudes are retained to achieve solutions of useful accuracy for a variety of geometric contributions. For an unloaded panel ($\lambda = 0$), the displacements degenerate into the imperfection shape of the panel:

$$\{u\} = q_i^0\{u_i\} + q_i^0 q_j^0\{u_{ij}\}, \qquad i, j = 1, 2, \ldots$$

where q_i^0 are the modal imperfection amplitudes that generate imperfections in the shapes of their respective buckling modes.

The assumed form of the displacements and the imperfection shapes are then used in the expressions for the midplane mechanical strains and curvatures. The governing equations are obtained by applying the principal of virtual work. Details for the methods of determining the linear unbuckled, the buckling, and the second-order displacement shape functions can be obtained from Ref. 2.

The design problem is to minimize the weight of a linked-plate panel such that it will sustain a specified design load N_D without an elastic limit load N_L failure or local material failure. In existing treatments of this problem,[1] the geometric imperfection is assumed to have a given shape, based on previous experience with the manufacturing process (Fig. 4). However, because of the nature of the manufacturing process, the actual shape of the geometric imperfection that is designed will be different from the assumed one and varies from panel to panel.

The objective is to introduce a convex model to account for the uncertainties in the imperfection profile of a manufactured panel. Thus, instead of using an estimate for a nominal imperfection profile in the design problem, an estimate for a number of imperfection parameters is used. These imperfection parameters are chosen so as to represent a realistic ensemble of panels that can be expected from the manufacturing process in hand. The output of the convex model is the weakest panel profile, which is then used in the design problem instead of the traditionally assumed nominal profile. A schematic of this process is shown in Fig. 5.

It is expected, however, that there is a close relationship between the design variables defining the stiffened panel, e.g., stacking sequences and dimensions, and the geometrical imperfections resulting in it after manufacturing. The investigation of this relationship and its incorporation in the design process are the main long-term objectives of this study. That is, in the long term we intend to close the loop with a manufacturing model that will account for the major

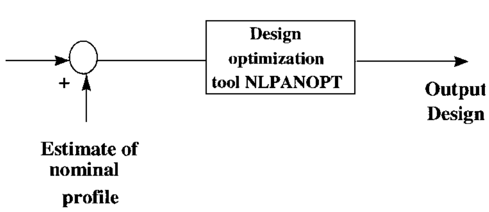

Fig. 4 Existing geometric imperfections treatment.

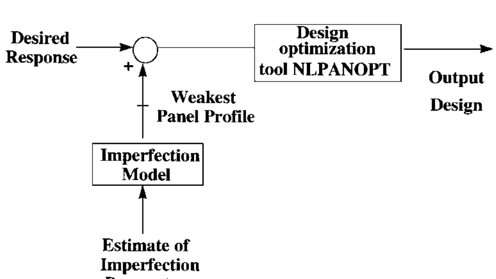

Fig. 5 Design process with imperfection model of uncertainties.

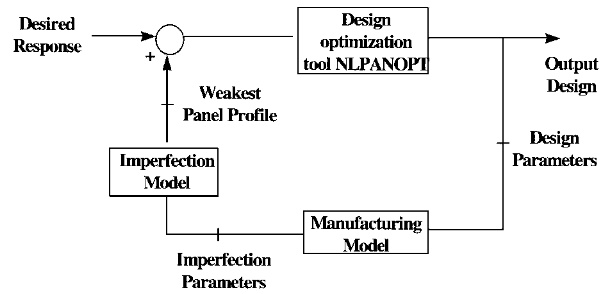

Fig. 6 Projected closed-loop design scheme.

sources of imperfections. The inputs to the manufacturing model are the design parameters defining the panel, e.g., dimensions and stacking sequences, and the outputs from it are the imperfection parameters that define the family of panels to be expected from the given manufacturing process. The imperfection parameters are then fed into the imperfection convex model to determine the weakest panel in the ensemble. The overall effect of this process is to reduce the effects of the geometric imperfections introduced by the manufacturing process on the final product to a minimum. The projected closed-loop design scheme is shown in Fig. 6.

III. Convex Models

The probabilistic approach to the modeling of uncertainty begins by defining a space of events and a probability measure on that space. The space is all inclusive; it includes everything that could occur and, possibly, events that cannot occur. The probability measure contains all information concerning the relative frequency of different events.

The set-theoretic (convex-model) approach to the modeling of uncertainty is different. A space of conceivable events is defined, as in the probabilistic approach. However, no probability measure is defined. Rather, sets of allowed events are specified, and the structure of these sets is chosen to reflect available information on what events can and cannot occur. It is remarkable, and of considerable practical significance, that sets whose elements represent spatial or temporal uncertainty are often found to be convex.[11] A region is convex if the line segment joining any two points in the region is entirely in the region. Circles and triangles delimit convex regions, whereas quadrilaterals may or may not, depending on whether their diagonals intersect within the region. In this paper, convex models are used to represent the uncertainty of the initial imperfection profile of the stiffened panel.

Let $\boldsymbol{q}$ be a vector whose components are the N dominant mode shape amplitudes in the representation of the initial imperfection profile of the stiffened panel. Furthermore, let $\eta(\boldsymbol{q})$ be the elastic limit load for a panel with initial imperfection profile $\boldsymbol{q}$. Let $\boldsymbol{q}^0$ be a nominal imperfection profile. Despite the uncertainties in many manufacturing parameters, panels that have been manufactured and handled under similar conditions are likely to experience forces that produce patterns of distortion common to all panels. Consequently, the average imperfection profile $\boldsymbol{q}^0$ is unlikely to be zero.

The elastic limit load for an arbitrary initial imperfection profile $\boldsymbol{q} = \boldsymbol{q}^0 + \boldsymbol{\xi}$, where $\boldsymbol{\xi}$ is a small deviation from the nominal $\boldsymbol{q}^0$, is given in first order in $\boldsymbol{\xi}$ as

$$\eta(\boldsymbol{q}^0 + \boldsymbol{\xi}) = \eta(\boldsymbol{q}^0) + \sum_{i=1}^{N} \left.\frac{\partial \eta}{\partial q_i}\right|_{q^0} \xi_i \tag{1}$$

In the present work, the deviation $\boldsymbol{\xi}$ from the nominal initial imperfection $\boldsymbol{q}^0$ is assumed to vary on the following ellipsoidal set:

$$Z(\alpha, \boldsymbol{\omega}) = \left\{\xi : \sum_{i=1}^{N} \frac{\xi_i^2}{\omega_i^2} \le \alpha^2\right\} \tag{2}$$

where the size parameter α and the semiaxes $\omega_1, \ldots, \omega_N$ are based on the experimental data available (or results of a computer simulation) for the manufacturing process. The components of the vector $\boldsymbol{\omega}$ are usually taken as the mean squared deviations from the average of the corresponding modal amplitude. Thus, $Z(\alpha, \boldsymbol{\omega})$ can be chosen to represent a realistic ensemble of panels. For all of the possible imperfection shapes that are contained in the convex set, we need to determine the weakest panel, i.e., the panel with the lowest elastic limit load. The lowest elastic limit that can be obtained in this ellipsoidal set Z can be expressed as

$$\mu(\alpha, \boldsymbol{\omega}) = \min_{\xi \in Z(\alpha,\omega)}[\eta(\boldsymbol{q}^0) + \varphi^T \boldsymbol{\xi}] \tag{3}$$

where

$$\varphi^T = \left(\frac{\partial \eta}{\partial q_1}\bigg|_{q^0}, \ldots, \frac{\partial \eta}{\partial q_N}\bigg|_{q^0} \right)$$

Note that $\boldsymbol{\xi}$ could also be assumed to vary in an n-box defined by the upper and lower bounds of its components, instead of an ellipsoidal set. (We call a Cartesian product of finite closed intervals an "n-box.") This would result in a weakest panel whose strength would be lower than that of the weakest panel obtained using an ellipsoidal set. Specifically, when using an n-box, we allow all of the components of $\boldsymbol{\xi}$ to assume their extreme values simultaneously. (This event corresponds to one of the vertices of the rectangular set.) The described event is very unlikely to occur because the uncertain parameters are usually statistically independent and, therefore, the weakest panel is likely to be too conservative. On the basis of this consideration, we chose an ellipsoidal set.

Equation (3) calls for finding the minimum of the linear functional $\varphi^T \boldsymbol{\xi}$ on the convex set $Z(\alpha, \boldsymbol{\omega})$. Based on inherent properties of a convex set, this extreme value will occur on the set of extreme points of the ensemble Z, i.e., the boundary of the ellipsoid, which is the collection of vectors $\boldsymbol{c} = (c_1, \ldots, c_N)$ in the following set:

$$C(\alpha, \boldsymbol{\omega}) = \left\{ c : \sum_{i=1}^{N} \frac{c_i^2}{\omega_i^2} = \alpha^2 \right\} \tag{4}$$

Thus, the minimum value of the elastic limit load in Eq. (3) becomes

$$\mu(\alpha, \boldsymbol{\omega}) = \min_{c \in C(\alpha,\omega)}[\eta(\boldsymbol{q}^0) + \varphi^T \boldsymbol{c}] \tag{5}$$

Define Ω as an $N \times N$ diagonal matrix whose nth diagonal element is $1/\omega_n^2$. Then, as seen from Eq. (4), we must minimize $\varphi^T \boldsymbol{c}$ subject to the constraint

$$f(\boldsymbol{c}) = \boldsymbol{c}^T \Omega \boldsymbol{c} - \alpha^2 = 0 \tag{6}$$

The method of Lagrange multipliers is used here. Define the Hamiltonian as

$$H(\boldsymbol{c}) = \varphi^T \boldsymbol{c} + \gamma f(\boldsymbol{c}) \tag{7}$$

where γ is a constant multiplier whose value must be determined. For an extremum, we require that the derivative of the Hamiltonian vanish:

$$\frac{\partial H}{\partial \boldsymbol{c}} = \varphi + 2\gamma \Omega \boldsymbol{c} = 0 \tag{8}$$

Thus,

$$\boldsymbol{c} = -(1/2\gamma)\Omega^{-1}\varphi \tag{9}$$

Substituting this into the constraint equation (6) yields the following expression for the multiplier:

$$\gamma^2 = (1/4\alpha^2)\varphi^T \Omega^{-1} \varphi \tag{10}$$

Backsubstituting for γ in Eq. (9), we find that the extremum deviation vector $\boldsymbol{c}$ is

$$\boldsymbol{c} = \pm \frac{\alpha}{\sqrt{\varphi^T \Omega^{-1} \varphi}} \Omega^{-1} \varphi \tag{11}$$

Thus, the minimum value of the elastic limit load is given by

$$\mu(\alpha, \boldsymbol{\omega}) = \eta(\boldsymbol{q}) - \alpha \sqrt{\varphi^T \Omega^{-1} \varphi} \tag{12}$$

Thus, to find the weakest panel profile, it is required to check only two panels given by

$$\boldsymbol{q}_1^* = \boldsymbol{q}^0 + \boldsymbol{c}, \qquad \boldsymbol{q}_2^* = \boldsymbol{q}^0 - \boldsymbol{c} \tag{13}$$

It is significant that the preceding analysis yields an explicit relationship between the minimum elastic limit load and the parameters defining the uncertainty in the initial imperfection α and $\omega_1, \ldots, \omega_N$.

In the next section, example problems are solved to validate the predictions of the convex model and to show the great reduction in effort and cost achieved by using a convex model instead of the traditional probabilistic analysis techniques.

IV. Validation of the Convex Model Predictions

To validate the convex model predictions for both the weakest panel profile and the minimum elastic limit load, a direct minimization problem is formulated as follows: Find $\boldsymbol{\xi}$ to minimize $\eta(\boldsymbol{q}) = \eta(\boldsymbol{q}^0 + \boldsymbol{\xi})$, subject to

$$\sum_{n=1}^{N} \frac{\xi_n^2}{\omega_n^2} \leq \alpha^2$$

Note that, as opposed to the convex model described in Sec. III (which considers only the boundary of the ellipsoid), the complete interior of the convex set constitutes the design space in this formulation. The outcome of this minimization problem is the profile of the weakest panel $\boldsymbol{\xi}^*$ in the family of panels described by the ellipsoidal constraint along with its corresponding minimum elastic limit load $\mu(\alpha, \boldsymbol{\omega})$. These are compared with the results of substituting for $\boldsymbol{q}^0$, α, and $\boldsymbol{\omega}$ into Eqs. (12) and (13) of the convex model.

Before solving the direct minimization problem that has just been described, a quick look at the function to be minimized shows that the response is highly sensitive to noise in numerical calculations. Thus, using a continuous minimization algorithm, e.g., conjugate gradient, might not lead to the required minimum. To smooth out the response, a response surface approximation for the actual function was employed. A single response surface was fitted around the point of zero imperfection using a central composite design with 324 function evaluations. However, low values of R^2 were obtained, which indicated that the surface did not provide a good fit for the variation in the elastic limit load. This is mainly due to the sudden switch in behavior around the origin that the response surface was not able to model. The panel under consideration has stiffeners only on one side of the skin and, hence, is asymmetric. Therefore, effects of the positive and negative imperfections on the response of the panel are quite different from one another. This suggested the use of two response surfaces: one for representing the region with negative q_1 (first mode amplitude) and the second for positive q_1 amplitudes. These surfaces were second-order polynomials, each requiring 257 function evaluations (designs).

We used stepwise regression to find the response surface polynomial.[12] This procedure removes redundant parameters from the approximating model, which is important in constructing an accurate and robust model. We used forward regression, which builds up an approximate model starting from the most important parameter and adding parameters to the model, one at a time, until there are no important parameters left. Tests that employ Mallows's Cp criterion, the partial R^2 criterion, or the partial F criterion can be used to identify the most important parameter in each step.[12] We used the partial F criterion as follows: In each step of the stepwise regression procedure, we have a model and a set of candidate parameters that can be added to the model. The value of F corresponding to each parameter measures the reduction in the sum of square errors of the model predictions that can be achieved if the parameter is included in the model. The parameter that has the largest F is considered as the most important parameter.

The quality of a model is measured using a quantity called R^2. This measures the portion of the variation in the actual response that the response surface model accounts for. A good model has typically an R^2 greater than 90%. The value of R^2 for the response surface corresponding to negative values of the first mode shape was 94.72%. This means that the response surface polynomial accounts for 94.72% of the variation in the elastic limit load. R^2 was 96.36% for the polynomial corresponding to positive values of the first mode shape. Figure 7 shows the variation of the elastic limit load with the first mode's amplitude q_1, as obtained from both the single and the two response surface approximations along with the exact variation. A good agreement is noticed, especially for values of q_1 away

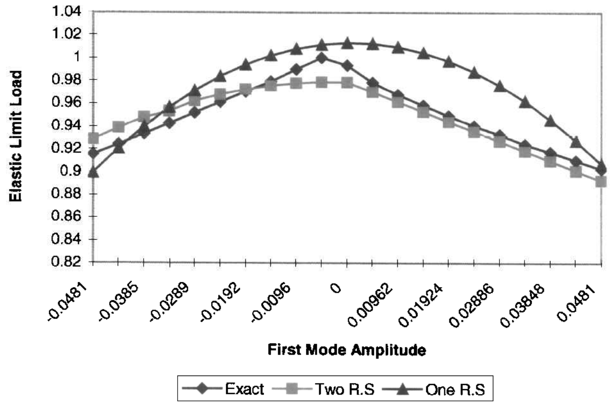

Fig. 7 Elastic limit load variation with first mode shape amplitude.

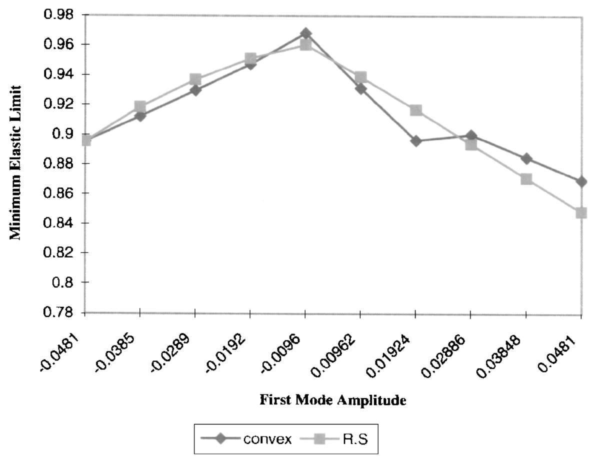

Fig. 8 Predictions of the convex model for the minimum elastic limit load, along with the minimum of the response surface.

from zero. Based on the preceding analysis, we concluded that the response surface polynomials were acceptably accurate.

The direct minimization problem is now reduced to the simple minimization of the quadratic response surface functions subjected to the ellipsoidal constraints.

The comparison is now performed for the following case:

$$q^0 = [-0.0481, 0.02104, 0.018037, 0.015031, 0.01202, 0.009018, 0.006012, 0.003006]$$

$$\alpha^2 = 8$$

$$\omega = [0.005879, 0.00514412, 0.00440925, 0.00367437, 0.0029395, 0.00220462, 0.00146975, 0.00073487]$$

A linear variation of the modal amplitudes was assumed, such that the first modal amplitude q_1 is set equal to its maximum value of 0.0481 in. and the ninth mode shape amplitude is assumed to be zero. Values of ω and α were obtained based on experience and general guidelines given by Ben-Haim and Elishakoff.[11]

To span the range of possible imperfection amplitudes, we move the center of the ellipsoid: The nominal value of the first mode's amplitude is varied from −0.0481 to 0.0481, whereas the amplitudes of the remaining modes are fixed. The predictions of the convex model are compared to the minimum of the response surface approximation. Figure 8 shows the predictions for the minimum elastic limit as q_1^0 is changed from −0.0481 to 0.0481. A very good agreement is observed.

The weakest panel shapes obtained from the two approximations are shown in Fig. 9 for the case $q_1^0 = -0.0481$. The mode shapes predicted by both the convex model and the response surface are so close that they are indistinguishable. Recall that the convex model

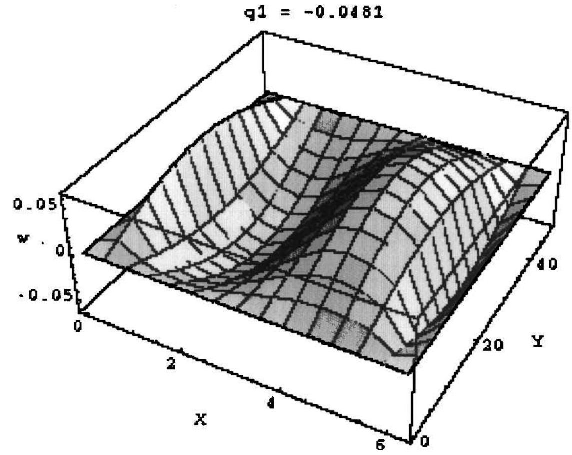

Fig. 9 Weakest panel shapes predicted by the convex model and the response surfaces.

predictions are obtained by simple substitutions in Eqs. (12) and (13). The construction of the response surface approximation, on the other hand, required the analysis of more than 500 panels to get a good fit to the actual variation.

V. Probabilistic Analysis of Elastic Limit of the Panel

In this section, the convex model is compared to a probabilistic model. There are three probabilistic approaches to a reliability assessment problem: 1) direct integration of the joint probability density function of the random variables over the failure region in the space of random variables, 2) second-moment methods, and 3) Monte Carlo simulation.

Direct integration is too expensive for problems involving more than three variables because it involves a nested integration. Therefore, it is not practical for most real-life problems. The main idea behind second-moment methods is to approximate the performance function with a simple function, which allows us to find the probability of failure using a closed-form, analytical expression.[13] The performance function is a function that is nonnegative if the structure survives and negative if it fails. The approximating function can be a first-degree or a second-degree polynomial. The polynomial can be determined using a Taylor series expansion of the performance function in the space of the random variables. The expansion point is called the most probable failure point or design point. It is determined by transforming the random variables into standard, independent Gaussian variables and finding the point on the limit state surface closest to the origin in the space of transformed variables. A standard Gaussian random variable has zero mean and unit standard deviation. The origin in the space or the transformed variables corresponds to the mean values of the original random variables. Optimization is used to determine the most probable failure point. Second-moment methods are far more efficient than direct integration and Monte Carlo simulation. They typically require fewer than 10 function evaluations (provided that closed-form analytical expressions for the sensitivities of the performance function with respect to the values of the random variables are available). An additional advantage is that they determine the sensitivity factors, which indicate the most important random variables. However, in a few cases, the optimization algorithm used for finding the most probable failure point may not converge or may converge to a local instead of a global optimum. In the latter case, the probability of failure can be grossly underestimated.

Monte Carlo simulation generates sample values of the random variables using a random number generator, calculates the performance function, and checks whether the structure fails. This procedure is repeated many times (from a few hundred to several thousand). The relative frequency of failure, i.e., the number of replications in which the structure has failed over the total number of replications, is an estimator of the failure probability. Monte Carlo simulation methods are easy to implement and robust but are also expensive. Therefore, they are used in cases where the performance function can be calculated rapidly. Some studies have approximated the performance function by a second-degree polynomial and performed Monte Carlo simulation using this polynomial instead of the performance function, which has reduced the computational cost dramatically.[14]

We did not use a second-moment method because the performance function describing the panel failure can have multiple most probable failure points. We used the second-degree polynomial presented in Sec. IV instead of the numerical analysis based on NLPAN for determining the panel elastic limit load, which reduced dramatically the computational cost of Monte Carlo simulation. Moreover, because the polynomial was found to approximate the actual elastic limit reasonably accurately, the estimated probability distribution of the elastic limit should also be accurate.

The coefficients that describe the deviations of the amplitudes of the modes from their nominal values were assumed to be independent and uniformly distributed random variables. They were assumed to vary in intervals defined by the axes of an ellipsoidal set (convex model). That is,

$$\xi_i \sim U(-\alpha\omega_i, +\alpha\omega_i), \qquad i = 1, \ldots, 8 \qquad (14)$$

where the values of α and ω_i are identical with those in Sec. IV. We considered 10 cases, where the nominal value of the first mode amplitude q_1^0 was assumed to vary between -0.0481 and $+0.0481$. The remaining mode amplitudes were assumed to be equal to 0.0001, and 100,000 replications were used.

Figures 10a and 10b compare the minimum elastic load found using the convex model and the 1 and 99 percentiles of the elastic load found using Monte Carlo simulation. The results of the convex and probabilistic models are in reasonably good agreement. Indeed, the minimum elastic load found from the convex model is quite close to the 1 percentile. However, the convex model predictions are not consistently below or above the 1 percentile. The probability of the elastic load predicted by the response surface polynomial being smaller than the elastic load predicted by the convex model ranged from zero, for $q_1^0 = -0.02886$, to 11.6%, for $q_1^0 = 0.03848$.

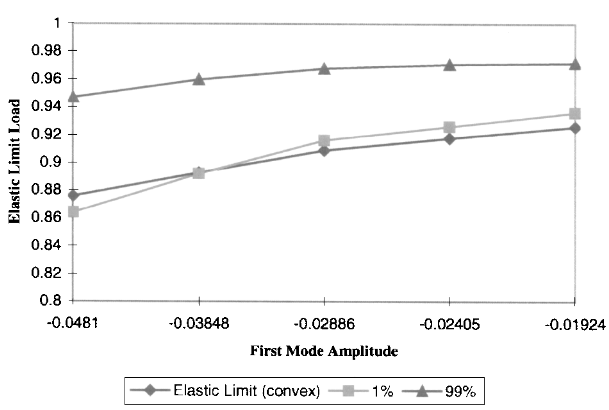

Fig. 10a Elastic limit load from the convex model and the probabilistic analysis for negative first-mode amplitudes.

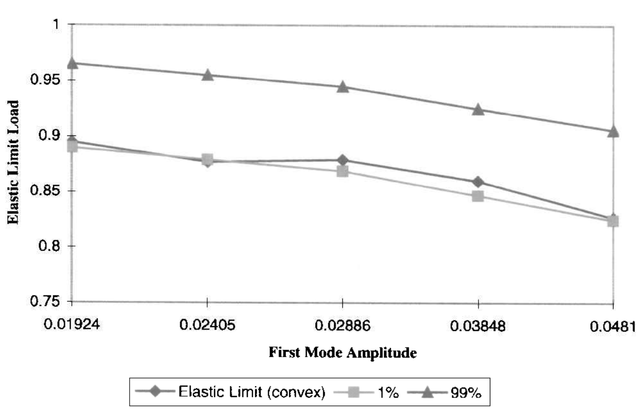

Fig. 10b Elastic limit load from the convex model and the probabilistic analysis for positive first-mode amplitudes.

This variation in the probability of not exceeding the convex model prediction should be due to 1) errors in the approximation of the elastic load by the second-order response surface polynomial and 2) noise in the numerical model used to predict the elastic load of the panel. The discontinuity in the convex model prediction of the minimum elastic limit load in Fig. 8 for $q_1^0 = 0.01924$ should also be because of numerical error.

For the example considered, the convex model appears to be adequate. The convex model requires less information about uncertainties and is considerably more efficient than probabilistic analysis. It does not require designs for fitting a response surface. Therefore, we decided to use it to reach the long-term objective of the study described in Sec. I.

In general, if little information about uncertainties is available, one should use a simple model that gives consistently conservative results. A convex model is likely to be better than a probabilistic model in these cases. However, a convex model that uses an ellipsoidal set to model uncertainties is not always conservative. For example, if some or all variables are strongly correlated, the probability of all of the variables assuming their extreme values simultaneously can be significant. In this case, the convex model that employs an ellipsoidal set can yield an unreasonably high characteristic value (that is, there is a significant probability that a sample panel has lower strength than the characteristic value). Therefore, in problems where the correlation between the random variables is not known, it is better to assume that the uncertain variables vary in an n-box instead of an ellipsoid.

VI. Conclusion

The objective was the development of a convex model for the uncertainties in the initial geometric imperfections of stiffened composite panels. We have demonstrated the suitability of the ellipsoidal linear convex model for the problem in hand. Significant cost and effort reductions have been achieved by the substitution of the more traditional probabilistic analysis by the convex model. The predictions of the convex model were compared to the results obtained by direct minimization. Good agreement was demonstrated for both the weakest panel profile and the minimum elastic limit load. Monte Carlo simulation has been performed, and convex model predictions were compared to those of the probabilistic analysis. The predictions of the two models were found to be quite consistent.

The long-term objective is the incorporation of the previously developed convex model of uncertainties together with a manufacturing model in the optimum design of the panels. The output of the manufacturing model will be values for $\boldsymbol{\omega}$, $\boldsymbol{q}^0$, and α. This information determines the family of panels that can be expected from the given manufacturing process. Feeding these parameters into the convex model yields the weakest panel shape in the ensemble. This imperfection shape should be used in the design instead of an assumed average shape. The overall effect of this process is the minimization of the effect of the initial geometric imperfection on the final product response and characteristics.

Acknowledgment

The research reported in this paper was sponsored by NASA Langley Research Center Grant NAG-1-643. The support is gratefully acknowledged.

References

[1] Perry, C. A., Gürdal, Z., and Starnes, J. H., Jr., "Minimum-Weight Design of Compressively Loaded Panels for Postbuckling Response," *Engineering Optimization*, Vol. 28, 1997, pp. 175–197.

[2] Stoll, F., Gürdal, Z., and Starnes, J. H., Jr., "A Method for the Geometrically Nonlinear Analysis of Compressively Loaded Prismatic Composite Structures," Center for Composite Materials and Structures, CCMS-91-03, Virginia Polytechnic Inst. and State Univ., Blacksburg, VA, Feb. 1991.

[3] Thompson, J. M. T., and Lewis, G. M., "On the Optimum Design of Thin Walled Compression Members," *Journal of Mechanical Physics of Solids*, Vol. 20, 1972, pp. 101–109.

[4] Bushnell, D., "PANDA2—Program for the Minimum Weight Design of Stiffened, Composite, Locally Buckled Panels," *Computers and Structures*, Vol. 25, No. 4, 1987, pp. 469–605.

[5] Wittrick, W. H., and Williams, F. W., "Buckling and Vibration of Anisotropic or Plate Assemblies Under Combined Loadings," *International Journal of Mechanical Science*, Vol. 16, 1974, pp. 209–239.

[6]Bolotin, V. V., “Statistical Methods in the Nonlinear Theory of Elastic Shells,” *Izvestiya Akademii Nauk SSSR*, Otdelenie Tekhnicheskikh Nauk, No. 3, 1958 (in Russian); also NASA TTF-85 (English translation), 1962, pp. 1–16.

[7]Budiansky, B., and Hutchinson, J. W., “Dynamic Buckling of Imperfection-Sensitive Structures,” *Proceedings of the 11th International Congress of Applied Mechanics*, edited by M. Gürtler, 1964, pp. 636–651.

[8]Elishakoff, I., “Hoff’s Problem in a Probabilistic Setting,” *Journal of Applied Mechanics*, Vol. 47, 1980, pp. 403–408.

[9]Lindberg, H. E., “Imperfection Uncertainty Control in Multi-Mode Buckling,” *Journal of Applied Mechanics* (submitted for publication).

[10]Ben-Haim, Y., and Elishakoff, I., “Non-Probabilistic Models of Uncertainty in the Non-Linear Buckling of Shells with General Imperfections: Theoretical Estimates of Knockdown Factor,” *Journal of Applied Mechanics*, Vol. 56, 1989, pp. 403–410.

[11]Ben-Haim, Y., and Elishakoff, I., *Convex Models of Uncertainty in Applied Mechanics*, Elsevier Science, Amsterdam, 1990.

[12]Draper, N. R., and Smith, H., *Applied Regression Analysis*, 2nd ed., Wiley, New York, 1981, pp. 307–311.

[13]Madsen, H. O., Krenk, S., and Lind, N. C., *Methods of Structural Safety*, Prentice–Hall, Englewood Cliffs, NJ, 1986, pp. 44–70.

[14]Fox, E. P., “Methods for Integrating Probabilistic Design Within an Organization’s Design System using Box–Behnken Matrices,” *Proceedings of the AIAA/ASME/ASCE/AHS/ASC 34th Structures, Structural Dynamics, and Materials Conference* (La Jolla, CA), AIAA, Washington, DC, 1993, pp. 714–723.

A. M. Waas
Associate Editor